TRITA-PFU-86-01

MULTIPOINT THOMSON SCATTERING SYSTEM FOR THE EXTRAP Z-PINCH EXPERIMENT

P. Karlsson

March 1986

Department of Plasma Physics and Fusion Research
Royal Institute of Technology
S-100 44 Stockholm, Sweden

MULTIPOINT THOMSON SCATTERING SYSTEM FOR THE EXTRAP Z-PINCH EXPERIMENT

P. KARLSSON

Royal Institute of Technology, S100 44 Stockholm, Sweden

ABSTRACT

A Thomson scattering system for simultaneous measurements of the electron temperature and density at three different positions at two different times during a single plasma shot has been developed for the EXTRAP-L1 Z-pinch. The plasma in the present version of EXTRAP-L1 is characterized by densities in the range from 10^{21} to 10^{22} m^{-3}, temperatures up to 50 eV and a pinch radius of the order of 1 cm. A spatial resolution down to 3 mm between positions is obtained by imaging the plasma onto an array of quartz optical fibres at the output slit of the spectrometer. Fifteen PM-tubes are used to detect the scattered radiation as well as the background radiation. Due to the relatively dense plasma prevailing in the present version of EXTRAP-L1 the number of scattered photons is large and the photon to electron conversion noise is small. The background radiation is the most important factor limiting the accuracy of the measurements.

1. Introduction

A Thomson scattering system has been designed to perform measurements of electron density and temperature on the EXTRAP-L1 device [1-3]. EXTRAP-L1 is a linear Z-pinch stabilised by an external octupole field generated by four conductor rods where the currents run antiparallell to the plasma current. In fig. 1 a cross section of the pinch is shown. In the EXTRAP experiment described in this report a glass tube liner has been inserted just inside the rods. The plasma that is generated in this version of EXTRAP-L1 is characterized by densities n in the range 10^{21} - 10^{22} m^{-3} and temperatures T up to 50 eV. Further the pinch diameter is estimated to be of the order of 1 cm and the duration of the discharge is around 80 μs. The present Thomson scattering system is capable of simultaneous measurements of the electron density temperature at three points across the pinch diameter at one axial position. The laser can be operated in a double pulse mode so measurements can be made at two different times during the discharge.

2. Theoretical background

When laser light scatters incoherently on electrons in a plasma the scattered power in the frequency interval $[\omega_s, \omega + d\omega_s]$ and in the solid angle $d\Omega$ can be expressed as [4]

$$P_s(\bar{R},\omega_s)d\Omega d\omega_s = \frac{P_\ell}{A} r_o^2 N \sin^2\psi f_{ek}\left(\frac{\omega_s-\omega_e}{k}\right) \frac{d\omega_s}{k} d\Omega \qquad (1)$$

where

ω_s = the angular frequency of the scattered radiation
ω_ℓ = the angular frequency of the incident radiation
$\bar{R}$ = the vector from the scattering volume to the point of observation
P_ℓ = the laser power
A = the cross section area of the laser beam
$r_o = e^2/4\pi\varepsilon_o m_e c^2$ is the classical electron radius (= 2.82×10^{-15}m)

N = the number of electrons in the scattering volume

ψ = the angle between the electric field if the laser radiation and the direction of the scattered radiation

$\bar{k} = \bar{k}_\ell - \bar{k}_s$ where $\bar{k}_\ell$ and $\bar{k}_s$ are the wave vectors of the incident and the scattered radiation respectively

$f_{ek} = \int\int_{-\infty}^{\infty} f_e(v_k, v_1, v_2)\, dv_1\, dv_2$ where

f_e is the distribution function for the electrons, v_k is the velocity component along $\bar{k}$, and v_1, v_2 are velocity components perpendicular to v_k.

SI-units will be used in this text unless otherwise stated. The amplitude of the scattered power increases with P_ℓ and N but is independent of A since $N = \langle n \rangle A L$ where $\langle n \rangle$ is the average electron density in the scattering volume and L is the length along the laser beam that is observed. From now on the brackets around n will be omitted. The amplitude is also affected by the angle ψ, maximum value obtained when the scattered light vector is perpendicular to the electric field of the laser light. The spread in frequency around the laser wavelength is determined by the electron distribution function for motions in the $\bar{k}$ direction.

Integrating Eq. (1) over the entire frequency spectrum we obtain

$$P_s(\bar{R})d\Omega = P_\ell\, n\, L\, r_o^2 \sin^2\psi\, d\Omega \qquad (2)$$

where the relation $\int_{-\infty}^{\infty} f_{ek} \left(\frac{\omega_s - \omega_\ell}{k}\right) \frac{d\omega_s}{k} = 1$ has been used. If the electrons have a Maxwellian distribution then

$$f_{ek} = 1/(v_{th}\sqrt{\pi}) \exp(-(v_k/v_{th})^2) \qquad (3)$$

where $v_{th} = \sqrt{\frac{2k_B T}{m_e}}$, k_B is the Boltzman constant and m_e is the

electron mass. Inserting Eq. (3) in Eq. (1) gives

$$P_s(R,\omega_s)d\omega_s d\Omega = \frac{P_\ell n L r_0^2 \sin^2\psi}{\sqrt{\pi} v_{th}} \exp\left[-\left(\frac{\omega_s-\omega_\ell}{kv_{th}}\right)^2\right]\frac{d\omega_s}{k} d\Omega \qquad (4)$$

If we restrict ourselves to a low temperature plasma, $v_{th} << c$ where c is the velocity of light, then $k = 4\pi \sin(\theta/2)/\lambda_\ell$ where θ is the angle between $\bar{k}_s$ and $\bar{k}_\ell$. This leads to

$$\frac{\omega_s-\omega_\ell}{kv_{th}} = \frac{c\Delta\lambda_s}{2v_{th}\lambda_\ell \sin(\theta/2)} \quad ; \quad d\omega_s = \frac{2\pi c}{\lambda_s^2} d\lambda_s \qquad (5)$$

which inserted in (3) becomes

$$P_s(R,\lambda_s)d\lambda_s d\Omega = \frac{P_\ell n L r_0^2 \sin^2\psi}{2\sqrt{\pi}\sin(\theta/2)} \frac{c}{v_{th}} \exp\left[-\left(\frac{c\Delta\lambda_s}{2v_{th}\lambda_\ell \sin(\theta/2)}\right)^2\right]\frac{d\lambda_s}{\lambda_\ell} d\Omega \qquad (6)$$

here λ_s = scattered wavelength and $\Delta\lambda_s = \lambda_s - \lambda_\ell$.

The wavelength spectra have a Gaussian shape with a full width at half maximum (FWHM) $(\Delta\lambda)_{1/2} = 2\sqrt{\ell n 2}\, v_{th}\lambda_\ell \sin(\theta/2)/c$. For θ = 90 deg and λ_ℓ = 6943 Å for a ruby laser we recognize $(\Delta\lambda)_{1/2} = 32.4\sqrt{T}$ Å, where T is given in eV.

The geometry of the laser light scattering is outlined in Fig.2. The laser beam enters the vacuum chamber in the horisontal plane and is forcused onto the plasma volume perpendicular to the pinch axis. The pinch has a radius a and the laser beam can be approximated by a cylinder with a diameter d through the pinch. The scattered photons are collected at an angle θ to the laser beam and over the solid angle $\Delta\Omega$ of the collection optics. The image of the entrance slit of the spectrograph, projected on to the horisontal plane, is a rectangle of length L along the laser beam and width Δz along the pinch axis. Is assumed that $\Delta z < d$.

If we integrate Eq. (2) over the duration of the laser pulse and divide by $h\nu_\ell$ (ν_ℓ is the laser frequency) we obtain the number of scattered photons

$$N_{ps} = (E_\ell/h\nu_\ell)\ r_o^2\ n\ L\ \sin^2\psi\ \Delta\Omega \tag{7}$$

E_ℓ denotes the laser pulse energy. It is assumed that the plasma quantities are constant during the laser pulse.

In the actual experiment the number of photons that is collected by the detection optics during the laser pulse, N_{pd}, can be expressed as

$$N_{pd} = N_{ps} + N_{pb} + N_{p\ell} \tag{8}$$

where N_{pb} is the number of background plasma photons and $N_{p\ell}$ is the number of photons originating from the laser stray light. This means that we must measure N_{pb} and $N_{p\ell}$ independently and deduct them from N_{pd}.

The fact that N_{pb} and $N_{p\ell}$ must be estimated by indirect measurements also introduces an error in determining N_{ps} as will be discussed later. We expect that N_{pb} will be much greater than $N_{p\ell}$ in our measurements. To get an order of estimate of N_{pb} we write

$$N_{sb} = n^2\ B(\lambda,T)\ \frac{\Delta t}{h\nu}\ \Delta\Omega\ \Delta\lambda\ \Delta V \tag{9}$$

Δt = the time interval of the measurement
n^2B=the radiated power per volume, wavelength and solid angle
ΔV = the volume from which plasma light is collected
$\Delta\lambda$ = the spectral width of the detected radiation

As a rough guideline we have taken the function $B(T,\lambda)$ from Reference [5] for the radiation from a fully ionised hydrogen like plasma:

$$B(T,\ ) = 0.166 \times 10^{-44} \frac{Z}{\lambda^2 T^{1/2}} \exp(-\frac{1.24 \times 10^{-6}}{\lambda T}) \qquad (10)$$

where T is given in eV. Taking the ratio N_{pb}/N_{ps} from (7), (9) we get

$$\frac{N_{pb}}{N_{ps}} = \frac{n\ a\ \Delta z}{E_\ell} \exp(-\frac{c_2}{T}) \qquad (11)$$

The constants are $C_1 = 5.6 \times 10^{-19}$ and $C_2 = 1.8$. We have assumed that we cover about 1/2 of the FWHM of the scattered spectrum with the detectors which yields $\Delta\lambda = 64.8\sqrt{T}\ 10^{-10}$ m, inserted $\Delta t = 10^{-7}$ s as the interval of detection and taken $\lambda \approx \lambda_\ell$. We see that in order to minimize this ratio it is advantageous to have large laser energy, low plasma density, small pinch radius and a small Δz. Taking typical parameter values $n = 10^{21}\,m^{-3}$, $T = 30$ eV, $z = 0.002$ m, $Z = 1$, $E_\ell = 7$ J and $a = 0.01$ m we obtain

$$\frac{N_{pb}}{N_{ps}} = 1.5 \times 10^{-3} \qquad (12)$$

This means that in the case of a hydrogen plasma with no impurities the background radiation is unimportant. However, the presence of impurities, e.g. oxygen, could change the picture.

The number of photons that, on the average reach one PM-tube is expressed as $\tau\ N_{pd}/m$, where τ is the transmission of the detection optics including reflection losses from the lenses, the transmittance of the spectrograph and the packing fraction of the fibre bundle and fibre matrix. The number of photoelectrons then is

$$N_e = \frac{\eta \tau N_p}{m} \qquad (13)$$

where η denotes the quantum efficiency of the PM-tube.

In our experiment θ = 67.5 deg, $\Delta\Omega$ = 0.01 sr, n = $10^{21} m^{-3}$, τ = 0.03, η = 0.07, E_ℓ = 7 J, m = 15, L = 0.01 m and Ψ = 90 deg are typical values of the parameters which inserted in Eq. (7) and Eq. (13) give $N_{es} = 2.7 \times 10^3$.

One of the determining factors in the uncertainty of N_p is the the statistical variation of the photoelectrons N_e. N_e is Poisson distributed with a standard deviation $\sigma = \sqrt{N_e}$. If N_{ps}, N_{pb} and $N_{p\ell}$ are independent and the stastistical noise is the only noise the then $\sigma_d^2 = \sigma_s^2 + \sigma_\ell^2 + \sigma_b^2$, where σ_k corresponds to N_{sk}, k = d,s,ℓ,b, and we thus obtain the signal to noise ratio

$$SNR = \frac{N_{es}}{\sqrt{N_{es}+2N_{eb}+2N_{e\ell}}} \qquad (14)$$

Here it is assumed that N_{pd}, N_{pb} and $N_{p\ell}$ are measured during a time interval of equal magnitude, Δt. Inserting the estimate of N_{es} above we obtain SNR = 2×10^{-2}. The noise due to the photon - electron conversion statistics should not be important in our case due to the relatively cold and dense plasma that exists in EXTRAP L-1.

3. Experimental set up

The experimental set up is shown on fig.3. First we have the laser input system consisting of the laser, input optics and stray light elimnination system. Then comes the detection system consisting of detection optics, spectrograph, detectors and data recording system.

3.1. Laser input system

A QUANTEL double pulse ruby laser is used giving 10 J in a single pulse of 20 ns or 2 x 7 J when operated in the double pulse mode. The divergence of the laser beam is less than 1 mrad. The interval between the pulses in double pulse mode can be set in the range 2-500 us. In Fig.3 we can follow the laser beam from the laser onto the pinch. The laser beam has a diameter of 16 mm when leaving the laser and is horisontally polarized. It undergoes a horisontal deflection by mirror M2 and is then magnified to a diameter of 24 mm by the lenses L1 and L2 before being deflected by mirrors M3 and M4. Although the average power density of the laser beam is almost one order of magnitude greater than the damage threshold of the mirrors, 3 GW/cm^2 for s-plane reflection, it is unevenly distributed over the beam cross section and could locally be over 1 GW/cm^2. The magnification of the beam reduces the power density by a factor of 2 thus increasing the safety margin of mirror destruction. Since the damage threshold for p-plane reflection is twice that of s-plane reflection no magnification is needed before M2. After M3 and M4 the beam is focused with L4 down to a diameter of 1 mm inside the pinch. The input quartz window is oprientated at the Brewster angle to minimize the reflection losses.

To reduce the stray light coming from scattering of the laser light on the input window a set of blueglass apertures are inserted between the input window and the pinch as shown in Fig.4a. This will prevent any incident radiation from hitting the wall of the vacuum chamber or the current rods: There are two holes of 10 mm diameter in the glass tube opposite each other to let the laser beam pass on to the beam dump. The beam dump simply consists of a vacuum quartz window and a blue glass plate orientated at Brewster angle. A further reduction of stray light entering the detection optics is obtained by installing a viewing dump opposite the collection lens as shown in Fig.4b. The design of the viewing dump has been taken from Ref. [6].

3.2. Detection system

A schematic view of the detection system is shown in Fig.3. A coherent quartz fiber bundle of 25 m length is used to transport the scattered light from the experimental hall out to an adjacent room where the detectors are protected from electromagnetic disturbances. The fibre bundle has an overall transmission of 50% and its ends have a rectangular shape, 1 x 5 mm^2 to fit the entance slit of the spectrometer. The end of the fibre bundle is imaged onto the pinch with a camera lens, f = 85 mm/1.8, to ensure low aberration. The lens and the fibre bundle are mounted inside a light tight, blackened brass tube. This arrangement permits a magnification of the fibre bundle end onto the plasma with a factor ranging from 1.35 to 3.0. The geometry of the vacuum vessel and the 4 current rods that create the octupole field determine the angle of collection and the solid angle of detection, θ = 67.5 deg and $\Delta\Omega$ = 0.07 sr.

The other end of the fiber bundle is imaged onto the entrance slit of the spectrometer with L5. The spectral dispersion is provided by a Monospek 1000, 1 m, f/9, plane grating spectrometer (Hilger and Watts). A 1200 1/mm grating is used with a blaze wavelength of 5000 Å which give a dispersion of 8.2 Å/mm. The input slit is 2 x 10 mm^2 and the corresponding etendue or throughput is T_{sp}=0.19 mm^2 sr. This is the lowest throughput of any part of the detection system thus setting an upper limit of the radiant flux in the system. Particularly it sets a limit of the solid angle $\Delta\Omega_{max}$ over which the plasma light is collected;

$$\Delta\Omega_{max} = \frac{T_{sp}}{A_{pl}} \qquad (15)$$

where A_{pl} = the area of the image of the fibre bundle onto the plasma. With the help of the lens formula we obtain an expression for the maximum F-number of the camera lens in order not to reduce the throughput of the system;

$$F_{max} = \sqrt{\frac{\pi A_{fb}}{4T_{sp}}} \frac{m}{1+m} \qquad (16)$$

where A_{fb} is the area of the fibre bundle, $p^2 = A_{pl}/A_{fb}$ and f is the focal length of the lens. Taking $p = 2$, which is the standard case in our measurements, gives $F_{max} = 3.5$ and in terms of the limiting solid angle we get $\Delta\Omega_{max} = 0.01$. This means that for the standard case $p = 2$ it is not the geometry of the vacuum vessel that limits $\Delta\Omega$ but rather the low throughput of the spectrograph.

The output slit of the spectrograph is imaged onto an array of 3 rows and 5 columns of optical quartz fibres each connected to a PM-tube. The fibres are 2 m long and have 1 mm diameter coated with a 0.1 mm thick cladding. The imaging element is a f=56 mm/1.6 camera lens and images the output slit onto the fibre array with an inverse magnification of 2.5:1. This arrangement permits a simultaneous measurement at 5 different wavelengths with a wavelength width of 25 Å and at three different points across the pinch with a separation of 3.3 mm. The stray light rejection ratio between two adjacent channels is measured to be 3×10^4.

The PM-tubes (Hammamatsu) employed are of the side on, multialkali cathode type with a cathode area large enough to capture the light emitted from the fibre without collection optics. We have employed two versions of the same PM-tube which differ regarding the cathode sensitivity and current amplification. R 928 has a quantum efficiency of 5% at 7000 Å and R 1477 has 8%, while the current amplification is typically 10^7 for R 928 and 5×10^6 for R 1477. The former is used where large proton flows scattered light is expected, i.e. the wavelength channels nearer to the laser wavelength and the latter is used where small photons fluxes are expected in order to improve the SNR due to the quantum statistical noise.

4. Data recording and evaluation

4.1. Calibration and stray light

A relative calibration of the channels was obtained by pulsing a light diode (Stanley 2K) having its maximum emission at 6600 Å with 50 ns pulses. The LED was placed in front of the plasma end of the fibre bundle and the spectrograph was adjusted so that every channel detected radiation at the same wavelength, 6800 Å. A relative calibration is sufficient for determination of the electron temperature.

In order to measure the density an absolute calibration is necessary which relates the magnitude of the signal to the number of scattering electrons. The standard procedure is to perform Rayleigh scattering on a Nitrogen gas. Since Rayleigh scattering does not change the wavelength of the laser radiation it is important that the stay light level is low. If the stray light is considerably greater than the Rayleigh scattered light an absolute calibration is impossible. In our case the stray light was found to be almost two order of magnitude greater than the Rayleigh scattered light. This is attributed to the glass tube surrounding the plasma since earlier measurements when the glass tube was not installed showed a stray light level comparable to the Rayleigh scattering at 5 torr nitrogen.

A relative measurement of the line integrated density is, however, possible. If we take Eq.(6) with $\Delta\lambda_s = 0$ we obtain;

$$P_s = C\, n\, P_\ell\, T^{-0.5} \qquad (17)$$

where C is a constant. Thus when the temperature has been determined and P_ℓ measured we can get a relative measurement of n.

4.2. Background plasma radiation

The plasma background radiation has been measured at different wavelengths and at several values of the external plasma parameters. The theoretical estimate presented earlier indicated that the background radiation was negligible compared to the scattered radiation. The measurements, however, show that for a range of external plasma parameters this is not the case so that a correction due to the influence of the background radiation is needed. The background plasma radiation will effect the measurement of the scattered radiation in 2 ways: First, as discussed before, the background photons will add to the measurement of the scattered photons. Second the background radiation could cause the saturation of the PM-tubes. The condition for our PM-tubes not to saturate is

$$\int_{t_o}^{t_s} i_a dt < 10^{-8}\ C \qquad (18)$$

where i_a is the anode current of the PM-tube, t_o is the time at which the plasma starts to form and t_s is the time at which the laser scattering occur. In our case it is only the first effect that is important.

To get a proper estimate of the background plasma radiation that has to be deducted one must either measure the background at a different time or at a different wavelength. In Fig.5, we show recordings of the background radiation for several plasma shots. The time scale of the recordings are the same but the calibration factors are not accounted for which means that the amplitudes are not comparable. The shape of the curves, however, contains information. Figures 5a and 5b show the background radiation recorded by the same channel at two different shots with the same external parameters. The shot to shot variation is seen to be significant. A comparison between Figs. 5a and 5c shows the spatial variation of the background radiation. Figure 5c is a recording for the same shot as Fig.5a and at the same wavelength interval but collects light from the central part of the plasma pinch while 5a looks at a part 3.3 mm away from the centre. Figures 5b and 5d illustrate

the wavelength dependence of the background radiation. They are recorded from the same shot and at the same spatial position but 50 Å apart.

The background radiation measurements show that it is preferable to measure this radiation at a different wavelength rather than 10 μs later in time. It is the data acquisition system that requires 10 μs to digitize the signals.

We choose to measure the background at a wavelength 125 Å from the laser wavelength where no scattered light appears. At each spatial point we use one channel to detect background radiation. A series of measurements of the background radiation only then gives a relative calibration between the 3 channels detecting background light and the 12 channels detecting scattered light with respect to the amount of background light.

4.3. Data Acquisition

The present experimental set-up allows measurements at 3 different positions and at 5 different wavelengths at each chord. It has been found that, in order to obtain sufficient accuracy in the determination of the electron temperature, measurement of scattered light at 4 different wavelengths is required. The fifth wavelength channel at each position is used for measuring the plasma background radiation since no scattered radiation has been detected there. The laser pulse energy varies from shot to shot and also needs to be measured if any information on the electron density is wanted. In order to measure the laser pulse energy a 400 μm quartz fibre is mounted behind the mirror M3, is shown in Fig.3, which samples and transmits the light to a silicon photo diode. A lens is used to ensure that the sample is a good average value.

There are thus a total of 16 signals that need to be registered at each measurement. The Thomson scattering system is connected to a CAMAC data acquisition system which is interfacing a LSI 11/23 computer. The signals from the PM-tubes are integrated and digitized by two LeCroy ADC 2250 CAMAC modules. The integration interval is specified by a gating pulse which is delivered by a pulse generator. The pulse generator is trigged by the signal from a photo

diode that detects the laser light that is transmitted through mirror M2.

A second measurement is possible 10 μs or more after the first when the laser is operated in the double pulse mode. It is the digitizing time of the ADC that sets the lower limit of the time interval between the pulses.

4.4. Data evaluation

The signal at each of the 16 channels, S_i, is proportional to the number of photons impinging on the photocathode,

$$S_{ki} = G_i \; e \; N_{eki} \qquad k=d,b,\ell \qquad i=1,15 \tag{19}$$

where the factors G_i are the current amplification factors of the PM-tubes and e is the electron charge. The signals $S_{i\ell}$ are measured without any plasma beeing present and the background signals S_{ib}, i = 1,12, is obtained from S_{id}, i = 13,15,as described in section 4.2. We thus obtain $S_{is} = S_{id} - S_{i\ell} - S_{ib}$. The temperature is obtained by fitting a straight line to $\ln(S_{is})$ vs $(\Delta\lambda_s)^2$. The interpolation of the straight line to $\Delta\lambda_s = 0$ then gives the average electron density according to Eq.(17).

5. Results

Because of the wide range of density in the experiments, the high voltage on the PMT:s must be adjusted to provide a good signal level. In order not to exceed the maximum rating, 256 pC, of the ADC:s the high voltage driving the PMT:s is lowered from 1000 V to 850 V. A typical signal due to the scattered light were found to be 200 pC when the PMT:s was operated at 850 V and taking G = 10^6 then gives N_{es} = 1.3 x 10^3. This is in accordance with the estimate made in section 2.

Results from a typical shot is shown in Fig.6. The data points are shown with error bars. The measurements of the background radiation showed that the shot to shot variation in the background level between the 3 channels employed to record background radiation and the other 12 channels was quite large. It has been found that this uncertainty gives the major contribution to the error bars.

Typically the measured intensity of background radiation is about two orders of magnitude greater than the estimate (12). This indicates that impurities must be present. Indeed, recordings of the H_α line,the line from the $3p^2D^o$ - $3d^2F$ transition in O II at 4705 Å and the background radiation at wavelengths of the scattered radiation during a shot shows a good correlation between the O II line and the background radiation. This correlation is not found between H_α and the background.

A reason for the large amplitude of the background radiation could be the glass tube isolating the plasma from the current rods. It is made of PYREX which contains significant proportions of metals which could serve as a radiation source. There are no holes in the glass tube between the collection optics and the viewing dump which enhances the radiative contribution from the glass tube.

6. Summary

A multichannel Thomson scattering system for EXTRAP-L1 has been developed. It is capable of simultaneous measurements of the electron temperature at three different positions and two different times during the discharge. The spatial resolution is 3.3 mm. The stray light level is too high for absolute calibration of the system, only permitting relative measurements of the electron density. This has been found to depend on the PYREX glass tube surrounding the plasma in the present version of EXTRAP-L1. A 1 m, f/9,plane grating spectrometer disperses the incoming radiation. The output slit of the spectrograph is imaged onto a 3 x 5 matrix of quartz optical fibres which provides the spectral and spatial resolution. The scattered photons and the background radiation are detected by 15 PM-tubes and for measuring the laser pulse energy a silicon photo diode is used. The detectors are connected to a CAMAC data acquisition system which evaluates the data after each plasma shot. The background radiation rather than noise from photon to electron conversion statistics has been found to be the greatest source of uncertainty in determining the electron temperature and density. Both theoretical and experimental investigations indicate that the background radiation originates from impurities.

7. Acknowledgements

The author is greatly indebted to Mr. J. Tonks for designing the interface between the plasma and the fibre bundle, as well as constructing the fibre matrix holder and numerous other mecano-optical components of the system. For introducing the author to the ruby laser and designing part of the laser beam guide Dr. B. Wilner is hereby thanked. Special thanks to Dr. J.R. Drake for valuable comments regarding the manuscript and to Mr S. Holmberg for writing part of the software for the data evaluation.

This work has been supported by the European Communities under an association contract between Euratom and Sweden.

References

[1] Lehnert, B., Physica Scripta 10, 139(1974)
Lehnert, B., Physica Scripta 16, 147(1976).

[2] Drake, J.R., Plasma Physics 26, 387(1984).

[3] Drake, J.R., Hellsten, T., Landberg, R., Lehnert, B., and Wilner, B., Plasma Physics and Controlled Nuclear Fusion Research 1980, Nuclear Fusion Suppl. II, 717(1981).

[4] Sheffield, J., Plasma scattering of electromagnetic radiation, Academic Press, New York, 1975.

[5] Lasalle, J., Platz, P., Plasma Physics 20, 107(1978).

[6] Desoppere, E., Van Oost, G, Bosia, G., Koch, R., Pearson, D., Laboratory Report No. 75, March 1981, Laboratoire de physique des plasmas, Ecole Royale Militaire, Brussels, Belgium.

Figure Captions

Fig.1. A cross section of the vacuum chamber.

Fig.2. The geometry of Thomson scattering.

Fig.3. Overview of the Thomson scattering system.

Fig.4. a) The laser stray light reduction system and beam dump.
b) The viewing dump and an enlarged drawing showing the details of the profile.

Fig.5. Plasma background radiation recordings.

Fig.6. A slightly modified computer output of the results from a typical shot. The logarithms of the signals are plotted vs $(\Delta\lambda_s)^2$ for three positions. Straight lines are fitted to the data points and the electron temperature and the relative electron density, $\tilde{n}_e$, are evaluated.

Fig.1

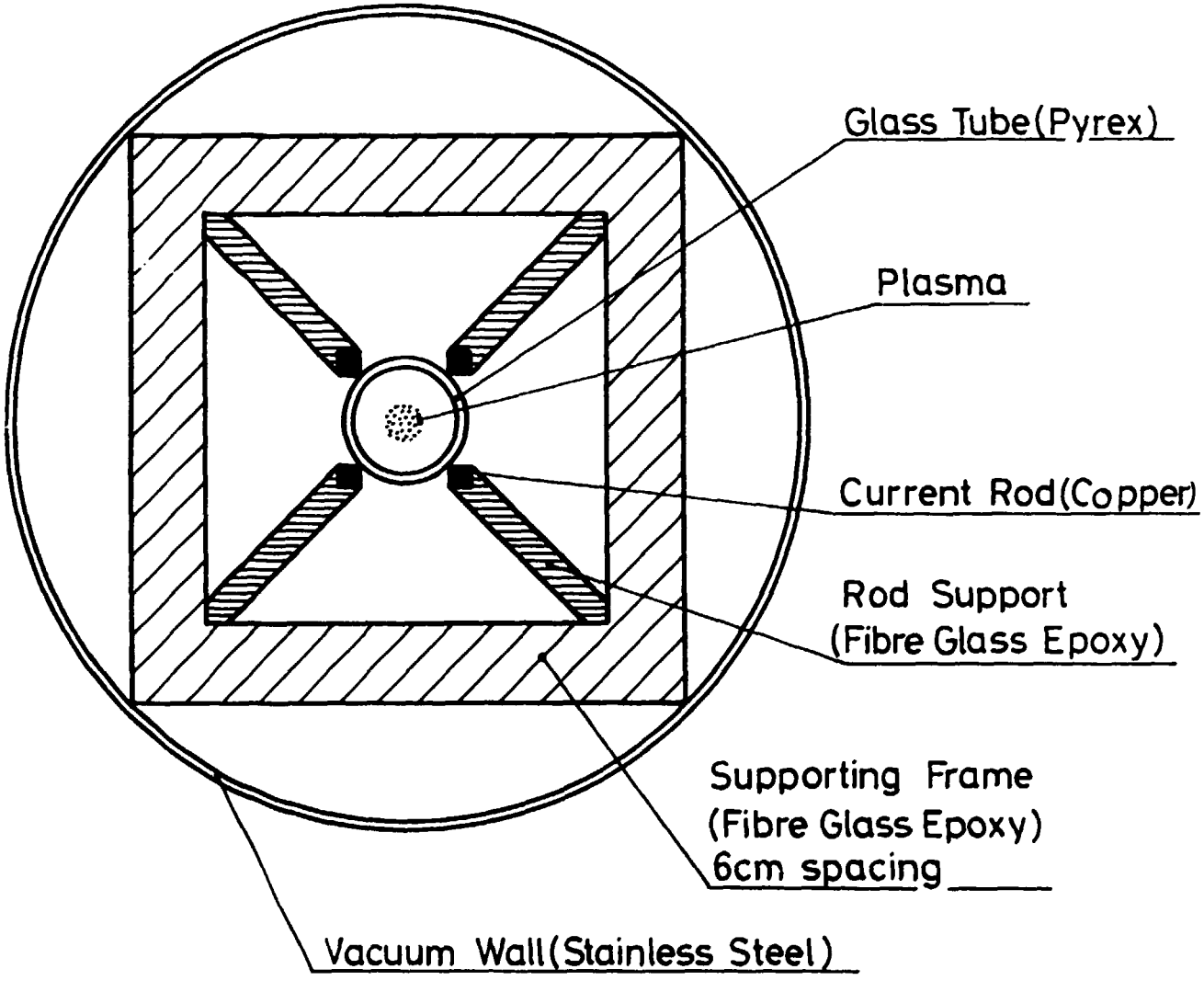
Glass Tube(Pyrex)
Plasma
Current Rod(Copper)
Rod Support
(Fibre Glass Epoxy)
Supporting Frame
(Fibre Glass Epoxy)
6cm spacing
Vacuum Wall(Stainless Steel)
10cm

Fig.2

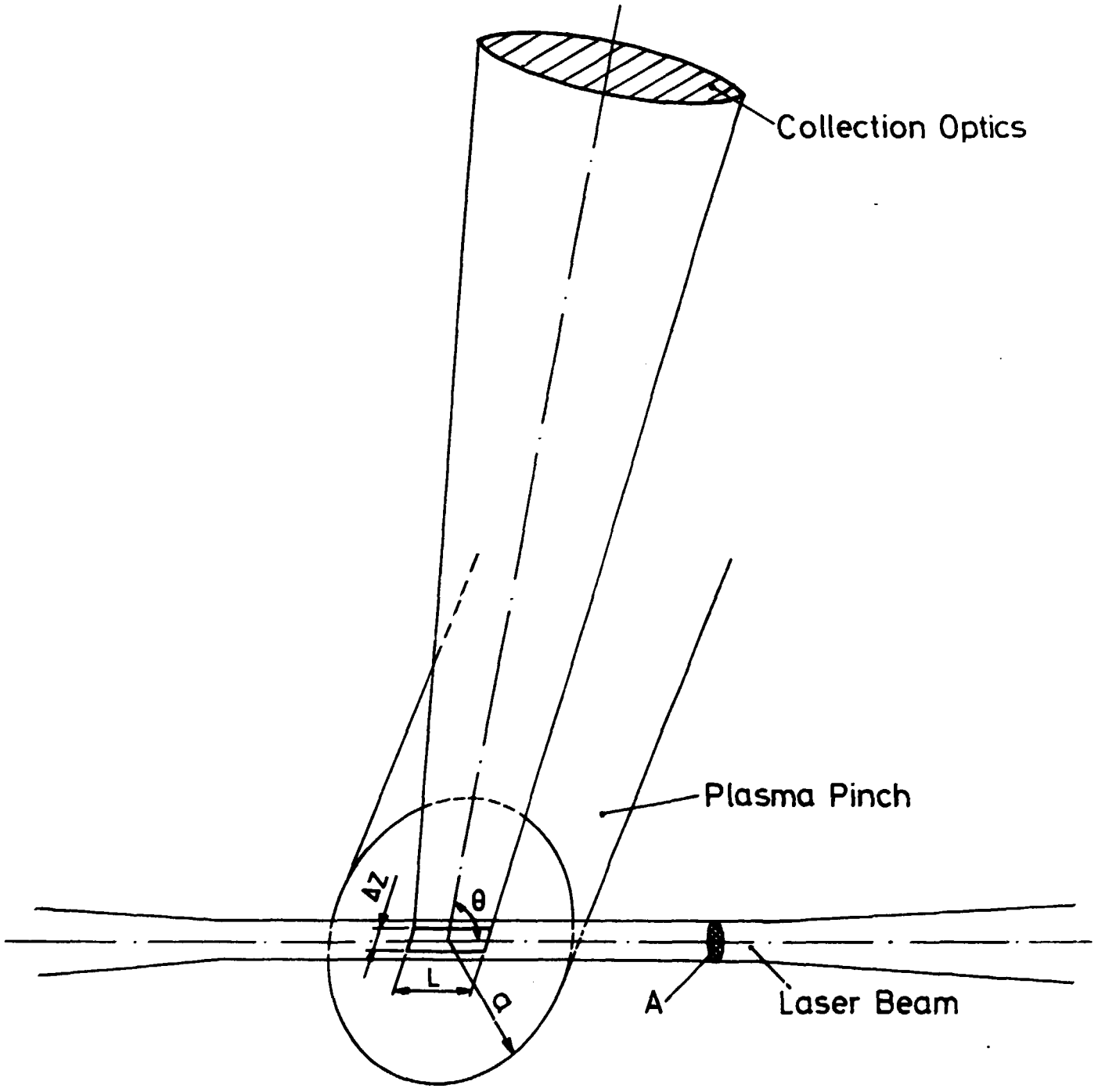

:Al-mirror
2-M4:High Energy Laser Mirrors
plano concave lens ; f=-200mm
plano convex lens ; f=300mm
plano convex lens ; f =15mm
plano convex lens ; f =1000mm
camera lens ; f=85mm / 1.8
camera lens ; f =50 mm / 1.4
camera lens ; f=58 mm / 1.8
=L3
Sheet polarizer

M(1)-PM(15): Photomultiplier Tubes
: Silicon Photodiode
2: Silicon Photodiode
V: High Voltage Power Supply
M: Fibre Matrix
D: Viewing Dump

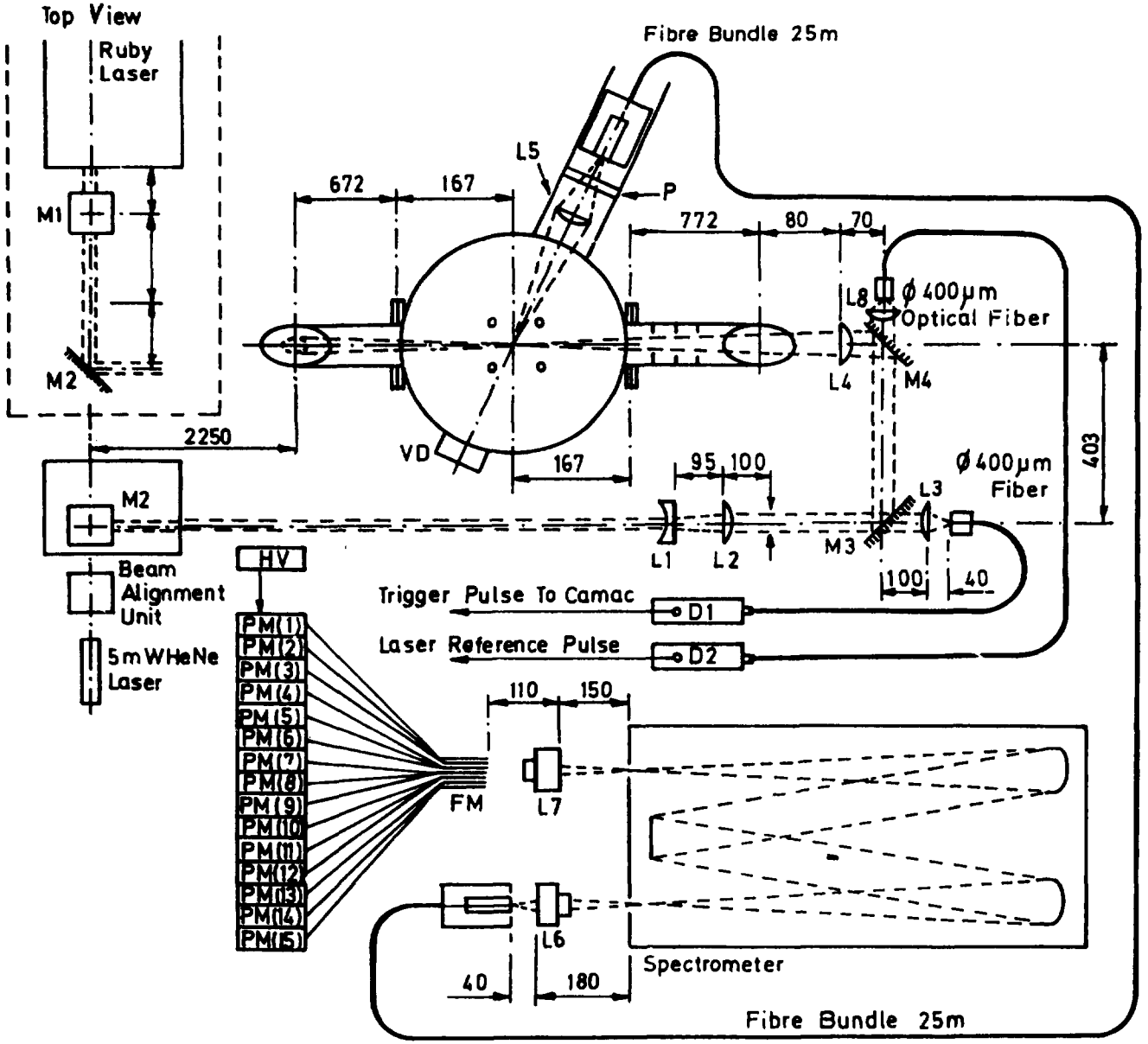

Fig.3

Fig.4

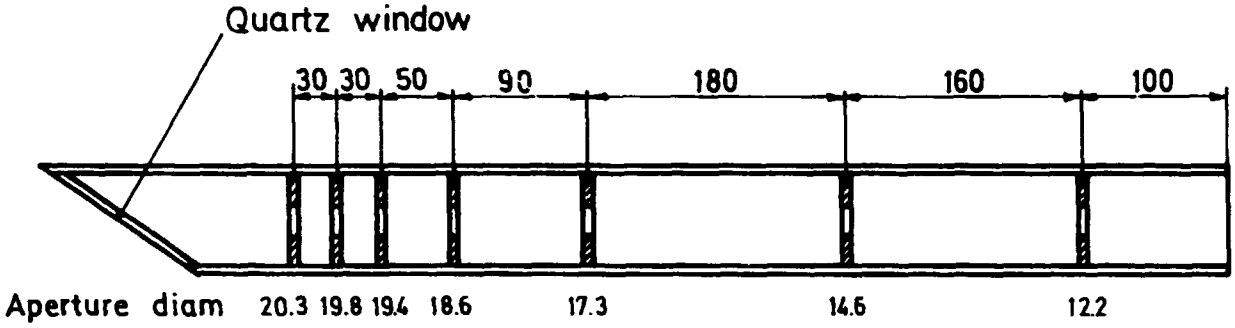

Direction of laserbeam

4a

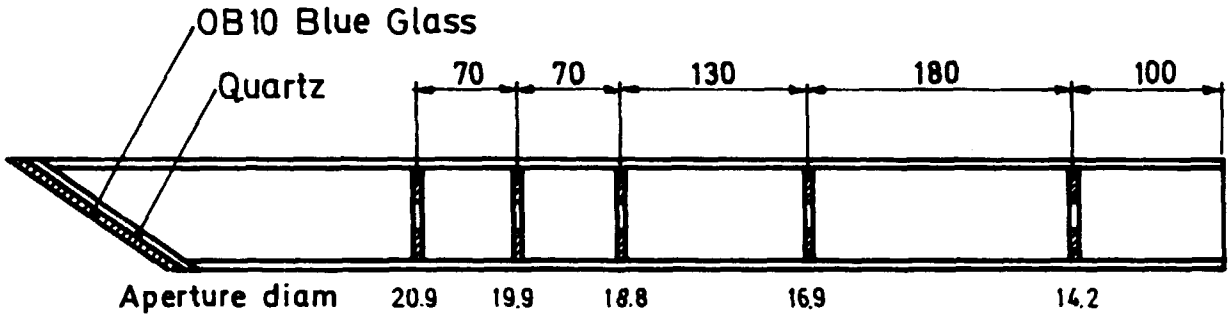

Direction of laserbeam

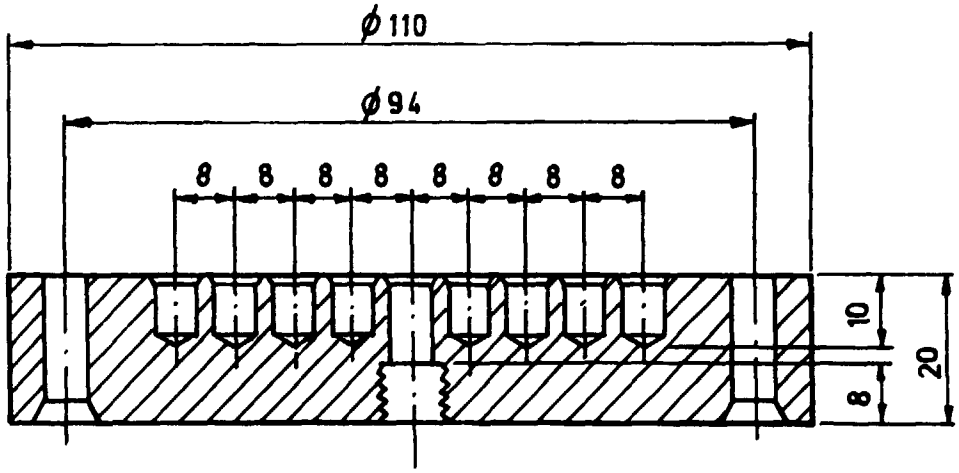

4b

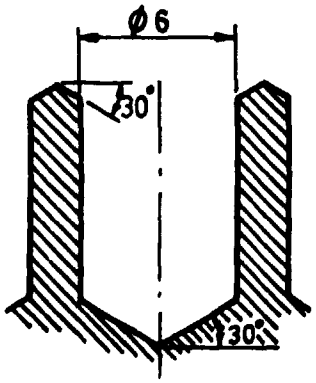

Fig.5

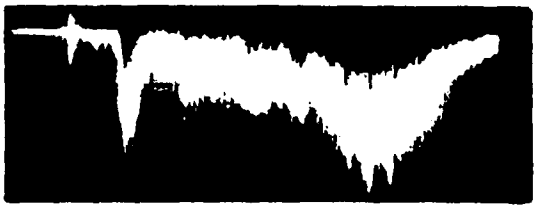

5a

5b

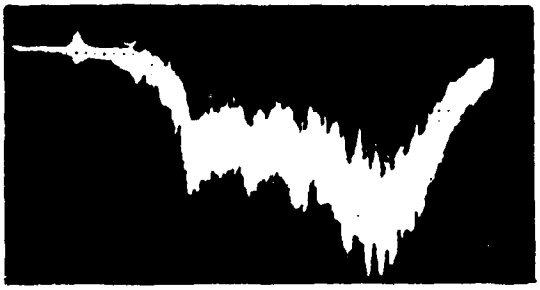

5c

5d

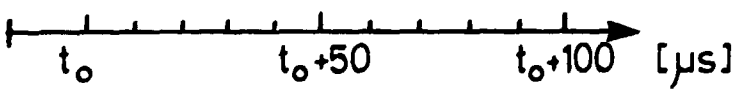

Shot # 1229 86-01-15 Fig.6

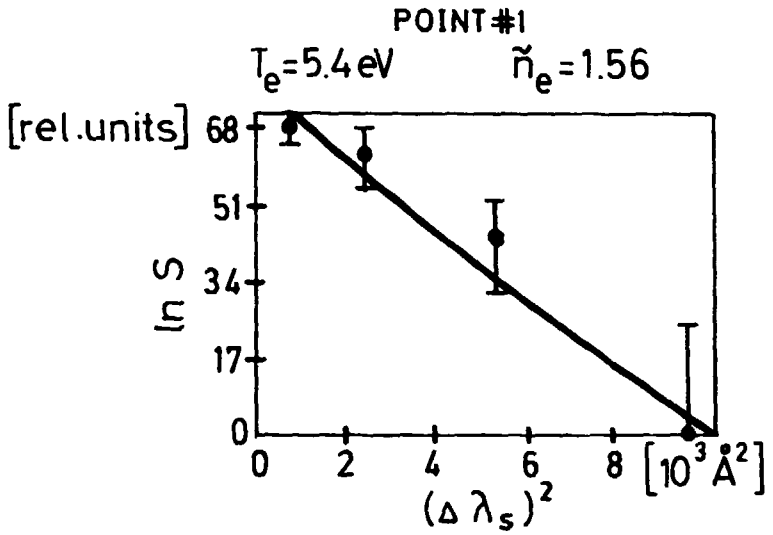

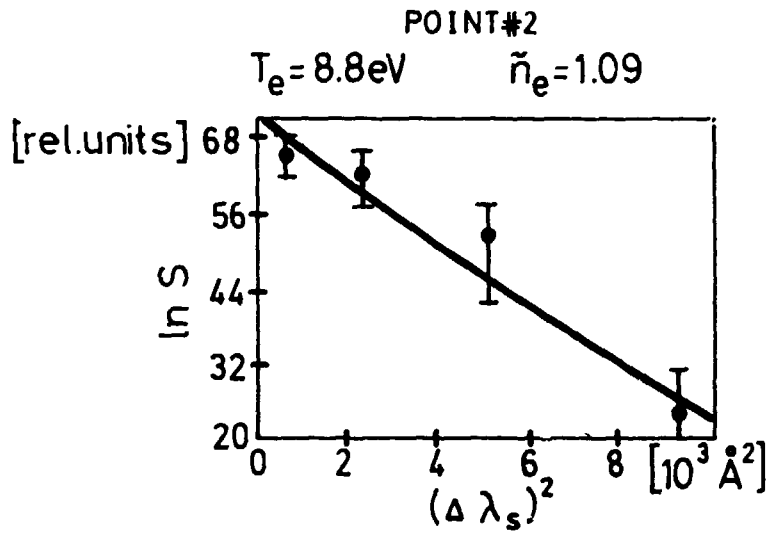

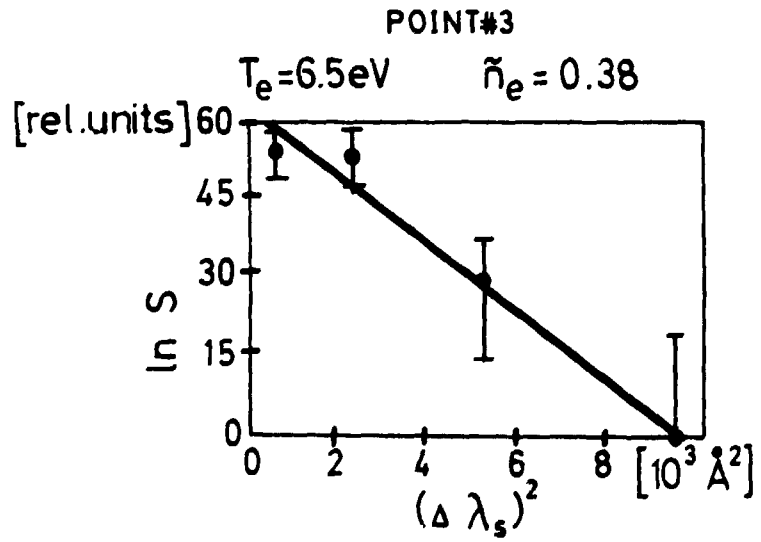

TRITA-PFU-86-01

Royal Institute of Technology, Department of Plasma Physics
and Fusion Research, Stockholm, Sweden

MULTIPOINT THOMSON SCATTERING SYSTEM FOR THE EXTRAP Z-PINCH EXPERIMENT

P. Karlsson, March 1986, 18 p. in English

A Thomson scattering system for simultaneous measurements of the electron temperature and density at three different positions at two different times during a single plasma shot has been developed for the EXTRAP-L1 Z-pinch. The plasma in the present version of EXTRAP-L1 is characterized by densities in the range from 10^{21} to 10^{22} m^{-3}, temperatures up to 50 eV and a pinch radius of the order of 1 cm. A spatial resolution down to 3 mm between positions is obtained by imaging the plasma onto an array of quartz optical fibres at the output slit of the spectrometer. Fifteen PM-tubes are used to detect the scattered radiation as well as the background radiation. Due to the relatively dense plasma prevailing in the present version of EXTRAP-L1 the number of scattered photons is large and the photon to electron conversion noise is small. The background radiation is the most important factor limiting the accuracy of the measurements.

Key words: Extrap Z-pinch, Thomson scattering, electron temperature, electron density